Basic Research in Cardiology (2018) 113:28
https://doi.org/10.1007/s00395-018-0685-y

ORIGINAL CONTRIBUTION

Cardiomyocyte dimethylarginine dimethylaminohydrolase1 attenuates left-ventricular remodeling after acute myocardial infarction: involvement in oxidative stress and apoptosis

Lei Hou[1] · Junjie Guo[2] · Feng Xu[3] · Xinyu Weng[1] · Wenhui Yue[4] · Junbo Ge[1]

Received: 1 November 2017 / Accepted: 29 May 2018 / Published online: 11 June 2018

Abstract

Asymmetric dimethylarginine (ADMA) is a risk factor for heart diseases. Dimethylarginine dimethylaminohydrolase (DDAH) enzymes are key proteins for ADMA degradation. Endothelial DDAH1 is a vital regulator of angiogenesis. DDAH1 is also expressed in cardiomyocytes. However, the role of DDAH1 in cardiomyocytes needs further clarification. Herein, we used an inducible cardiac-specific DDAH1 knockdown mouse (cardiac DDAH1$^{-/-}$) to investigate the role of cardiomyocyte DDAH1 in left-ventricular (LV) remodeling after acute myocardial infarction (AMI). DDAH1flox/flox and α-MHC^{MerCreMer} mice were used to generate cardiac DDAH1$^{-/-}$ mice. Deletion of DDAH1 in cardiomyocytes was confirmed by Western blotting. No significant differences were observed in plasma ADMA levels and LV function between cardiac DDAH1$^{-/-}$ mice and control mice. Cardiac DDAH1$^{-/-}$ mice showed aggravated LV remodeling 4 weeks after AMI, as demonstrated by a large infarct area and impaired LV function. The rate of cardiomyocyte apoptosis and level of oxidative stress were higher in the LV tissue of cardiac DDAH1$^{-/-}$ mice than in that of control mice. However, treatment of cardiomyocytes with exogenous ADMA had no effect on reactive oxygen species (ROS) levels or apoptosis sensitivity. Cardiac DDAH1$^{-/-}$ LV tissue showed downregulated superoxide dismutase2 (SOD2) expression, and treatment of DDAH1$^{-/-}$ cardiomyocytes with the SOD mimic tempol significantly attenuated apoptosis and ROS levels under hypoxic conditions. Tempol administration also attenuated oxidative stress and apoptosis in cardiac DDAH1$^{-/-}$ LV tissue and partially alleviated LV remodeling after AMI. DDAH1 in cardiomyocytes plays a vital role in attenuating LV remodeling after AMI by regulating intracellular ROS levels and apoptosis sensitivity via a SOD2-dependent pathway.

Keywords Dimethylarginine dimethylaminohydrolase · Acute myocardial infarction · Left-ventricular remodeling · Apoptosis · Reactive oxygen species

Introduction

Heart failure secondary to acute myocardial infarction (AMI) remains a clinical challenge despite the advances in medical and interventional therapy in recent decades [19]. Left-ventricular (LV) remodeling plays a major and important role in the progression from AMI to heart failure with

Lei Hou, Junjie Guo, and Feng Xu have contributed equally to this work.

Electronic supplementary material The online version of this article (https://doi.org/10.1007/s00395-018-0685-y) contains supplementary material, which is available to authorized users.

✉ Junbo Ge
ge.junbo@zs-hospital.sh.cn

[1] Department of Cardiology, Shanghai Institute of Cardiovascular Diseases, Zhongshan Hospital, Fudan University, Shanghai, China

[2] Department of Cardiology, The Affiliated Hospital of Qingdao University, Qingdao, Shandong, China

[3] Scientific Research Department, Shanghai Ninth People's Hospital, Shanghai Jiao Tong University, School of Medicine, Shanghai, China

[4] Department of Cardiology, Pan-Vascular Research Institute, Shanghai Tenth People's Hospital, Tongji University School of Medicine, Shanghai, China

respect to both geometry and function [4, 9]. Thus, it is essential to identify novel targets to prevent LV remodeling after AMI.

Asymmetrical dimethylarginine (ADMA) is a risk factor for heart disease [1, 3]. Dimethylarginine dimethylaminohydrolase (DDAH) enzymes are key proteins for ADMA degradation. The previous studies have shown that global deletion of DDAH1 significantly elevates plasma ADMA levels, which lead to reduced nitric oxide production and elevated blood pressure [12]. Recently, Dowsett et al. showed impaired angiogenesis potential without an increase in the level of ADMA in the plasma of endothelium-specific DDAH1 knockout mice [5], which indicated that tissue-specific DDAH1 might exert other effects independent of ADMA degradation. DDAH1 is also expressed in cardiomyocytes, and whether DDAH1 in the cardiomyocytes can protect the ischemic heart from LV remodeling after AMI remains unknown.

In this study, we showed that LV remodeling was more severe in cardiac DDAH1$^{-/-}$ mice than in control mice after AMI and that there was no increase in the plasma ADMA level. Furthermore, we found that DDAH1 plays a fundamental role in AMI-induced LV remodeling by regulating the reactive oxygen species (ROS)level and apoptosis sensitivity in cardiomyocytes via an SOD2-dependent pathway.

Methods

Induction of a cardiomyocyte-specific DDAH1 KO mouse

DDAH1$^{flox/flox}$/α-MHC^{MerCreMer} (referred to as cardiac DDAH1$^{-/-}$ mice hereafter) and DDAH1$^{flox/flox}$ (referred to as WT mice hereafter) mice were generated as previously reported [28]. Briefly, 4-hydroxytamoxifen (Sigma-Aldrich) was administered for 12 days by intraperitoneal injections (20 mg/kg/day) (Fig. 1a).

Experimental design and treatment

In the first part of the animal experiments, 12-week-old mice were divided into two groups (WT group and cardiac DDAH1$^{-/-}$ group). Structural and functional tests were performed 4 weeks after AMI. In rescue experiments, 12-week-old mice were assigned to four groups. WT mice and cardiac DDAH1$^{-/-}$ mice received either tempol or water from the day of the AMI procedure until 4 weeks after AMI. Tempol (Sigma-Aldrich) was administered at a dosage of 1.5 mmol/kg/day in the drinking water as described in a previous study [6]. There was no significant difference in the intake of water among subgroups. The experimental studies in mice were

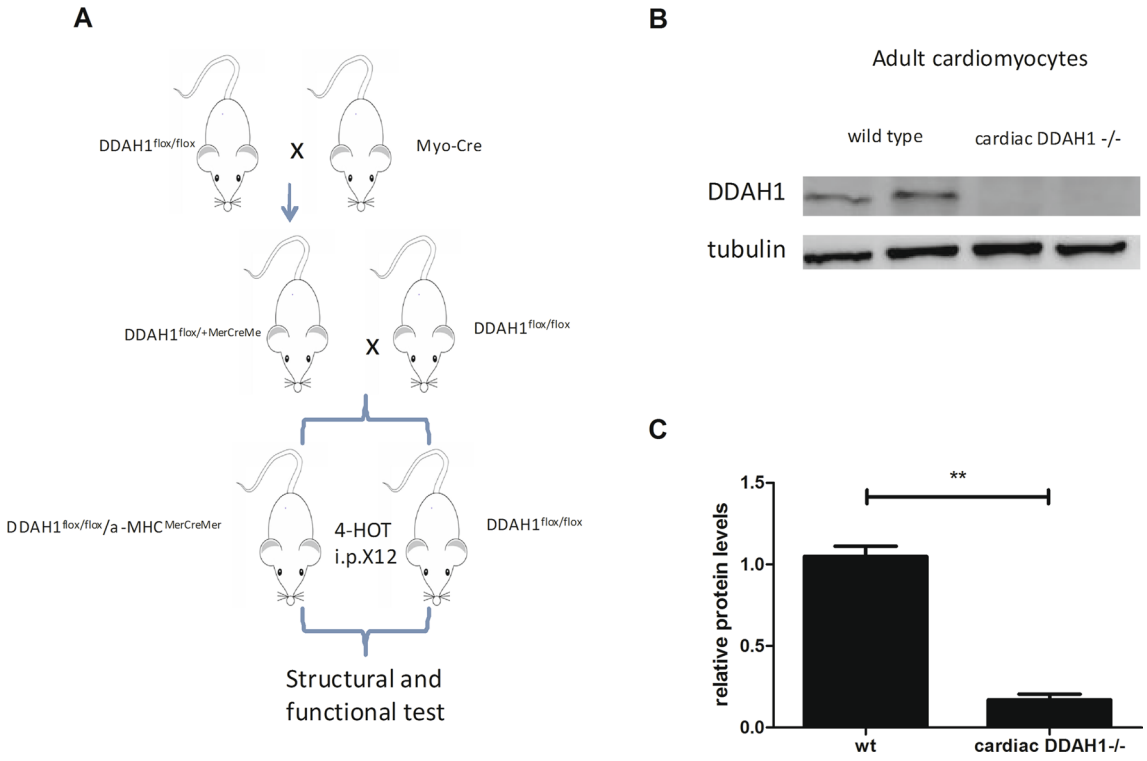

Fig. 1 Generation of cardiac DDAH1 $^{-/-}$ mice. **a** Diagram shows the approach to generating cardiac DDAH1$^{-/-}$ mice. **b**, **c** Western blot analysis shows reduced DDAH1 expression levels in isolated adult cardiomyocytes; $^{**}p < 0.01$

approved by the Ethics Committee of Animal Experiments in Zhongshan Hospital of Fudan University and performed according to institutional guidelines.

Primary cardiomyocyte culture

Ventricles from 2-day-old wild-type mice or global DDAH1$^{-/-}$ mice (kind gift by Professor Yinjie Chen from the University of Minnesota, USA) were dissected and minced. Then, the tissue was digested overnight at 4 °C with 0.5% trypsin (Thermo Fisher Scientific) in Ca^{2+}- and Mg^{2+}-free Hank's balanced salt solution. Then, the tissue was warmed and kept at 37 °C in 0.1% collagenase type 1 (Sigma-Aldrich) for 30 min. After passage through a 100-µm mesh, the solution was centrifuged at 500×*g* for 5 min and resuspended in culture medium with 10% fetal bovine serum (FBS; Thermo Fisher Scientific). Cells were seeded two times on plates coated with 1% collagen (Thermo Fisher Scientific) to remove fibroblasts. Subsequently, cells were centrifuged, resuspended, and seeded on 1% collagen-coated dishes. Hypoxia was achieved by placing the cells in a hypoxia incubator (STEMCELL Technologies) filled with 5% CO_2-nitrogen balanced gas mixture with a final oxygen level of < 1% inside the chamber.

Surgical procedure

After anesthesia with 2% isoflurane, mice were fixed on a heating pad. The left coronary artery was ligated approximately 3–4 mm from the origin, and AMI was confirmed by ST-segment elevation in the electrocardiogram. For the sham group, mice were subjected to the same procedure without ligation.

Measurement of cardiac function

Echocardiographic images were obtained with a VisualsonicsVevo System (Visual Sonics Inc, Canada). The mice were anesthetized, and the heart rates were maintained between 450 and 500 beats per minute. Both B- and M-mode images were acquired, and the left-ventricular internal diastolic diameter (LVIDD), left-ventricular interval systolic diameter (LVIDS), left-ventricular ejection fraction (EF), and left-ventricular fractional shortening (FS) were measured as previously described [7]. All measurements were completed by two blinded experienced technicians. A total of 10–12 mice were analyzed per group.

Determination of plasma ADMA concentrations

Plasma ADMA was detected using the ADMA direct ELISA Kit (Enzo Life Sciences) according the product manual provided by the manufacturer. Samples from ten mice were analyzed per group.

Histopathological examination of mouse hearts

The left ventricle was sliced from the apex to the base at 6-µm thickness for the evaluation of morphology and interstitial fibrosis. Sections were stained with Masson's trichrome. The infarct size was expressed as the infarct area relative to the total LV area. The percentage of LV fibrosis was determined using a previously described method [23]. Samples from six mice were analyzed per group.

Proteome analysis of LV tissue from cardiac DDAH1$^{-/-}$ mice compared with that from WT mice

Approximately 200 µg of total protein from fresh LV tissue of WT or cardiac DDAH1$^{-/-}$ mice 4 weeks after AMI was proteolyzed as previously described [22].

Each sample was analyzed three times by label-free, relative quantitative analysis. LC separations were conducted on the EASY nano-LC system (Thermo Fisher Scientific GmbH, Bremen, Germany).

All files from MS runs were analyzed using MaxQuant software (version 1.3.0.5) with minor modifications. The protein quantification results from the 'proteinGroups.txt' files were further analyzed by Perseus software (version 1.5.1.6). Proteins were defined as differentially expressed if the ratios were ≥ 1.3 or ≤ 0.77 in LV tissue from WT compared with LV tissue from cardiac DDAH1$^{-/-}$ mice and the change was statistically significant ($p < 0.05$).

Hierarchical clustering was completed using MEV software (v4.6, TIGR). The differentially expressed proteins were analyzed to find potential markers to classify all samples. Samples from three mice were analyzed per group.

Western blotting

Total protein was extracted from homogenized heart tissue using a complete protease inhibitor cocktail and RIPA Lysis-Buffer (Beyotime Biotechnology, Nanjing, China). Subsequently, 50 µg of protein was resolved by 10 or 12% sodium dodecyl sulfate-polyacrylamide gel electrophoresis (SDS-PAGE) based on the molecular weight of target proteins and was transferred to polyvinylidene fluoride (PVDF) membranes. Protein expression was detected by immunoblotting with antibodies against DDAH1 (SAB) and SOD2 (USCN Life Science); 3-nitrotyrosine(abcam)and tubulin (Sigma-Aldrich) served as the loading control. After three washes, the blots were incubated with the corresponding secondary antibodies (Sigma-Aldrich), and the immunoreactive bands were visualized by chemiluminescence and quantified using Image-Pro

Plus software (Media Cybernetics,Maryland, America). Samples from six mice were analyzed per group.

Detection of ROS

The level of superoxide was determined by spectrophotometry using dihydroethidium (DHE). The cultured cells were washed with phosphate-buffered saline (PBS) and incubated with 5 μM fluorescent dyes at 37 °C according to the manufacturer's instructions. Then, the cells or frozen sections were washed three times and imaged using fluorescence microscopy (Nikon, Tokyo, Japan). Fluorescence intensity was determined using Image-Pro Plus software (Media Cybernetics, Maryland, America). The results were from three independent experiments.

The level of superoxide in LV tissue was also determined by spectrophotometry using dihydroethidium (DHE) as described above. Samples from six mice were analyzed per group.

Apoptosis assay

Apoptosis of cells was measured by flow cytometry. Cultured cells were harvested and resuspended in binding buffer and incubated with AnnexinV-FITC and propidium iodide (PI) (BD Biosciences, USA) at room temperature for 15 min protected from light. Then, the samples were analyzed using FACS Calibur (BD Biosciences, USA). The results were from three independent experiments.

LV tissue sections were incubated with terminal deoxynucleotidyl transferase-mediated dUTP nick end labeling (TUNEL) reaction mixture for 1 h and stained with 4′,6-diamidino-2-phenylindole (DAPI). TUNEL-positive cells were counted in six random fields and recorded as a percentage of all nuclei. Samples from six mice were analyzed per group.

Statistical analysis

All values are expressed as the mean ± standard error. Data from two groups were compared using unpaired *t* test. Two-way ANOVA was used to test for differences between KO and wild-type animals under control conditions and after AMI. Post hoc pair wise comparisons were made using Fisher's least significant difference test. A value of $p < 0.05$ was considered statistically significant.

Results

DDAH1 expression level was reduced in cardiomyocytes from cardiac DDAH1$^{-/-}$ mice

The DDAH1 expression level was reduced by approximately 80% in cardiomyocytes isolated from cardiac DDAH1$^{-/-}$mice compared to those isolated from WT mice ($p < 0.01$) (Fig. 1b, c).

Cardiac-specific DDAH1 knockdown had no detectable effect on LV structure and function in mice

At baseline, cardiac DDAH1$^{-/-}$ and WT mice (12 weeks old) showed no significant differences in cardiac geometry and function (Table S1). Both strains shared a similar heart weight, LV weight and their ratios to body weight under baseline conditions. Echocardiography demonstrated that induced cardiac-specific DDAH1 knockout (KO) had no detectable effect on the EF (0.66 ± 0.04 in WT vs. 0.65 ± 0.05 in cardiac DDAH1$^{-/-}$ mice), LVIDS (2.96 ± 0.28 mm in WT vs. 3.15 ± 0.13 mm in cardiac DDAH1$^{-/-}$ mice), and LVIDD (4.13 ± 0.10 mm in WT vs. 4.17 ± 0.13 mm in cardiac DDAH1$^{-/-}$ mice) (Table S1) in mice under baseline conditions.

DDAH1 deficiency aggravated cardiac remodeling and dysfunction after AMI

Four weeks after AMI, cardiac DDAH1$^{-/-}$ mice exhibited worse pathological cardiac remodeling and dysfunction than control mice.

Histological examination demonstrated that DDAH1 deficiency resulted in a large infarcted size (48.5 ± 4.5% in WT vs. 62 ± 3.7% in cardiac DDAH1$^{-/-}$ mice, $p < 0.01$) (Fig. 2a, e) and enhanced fibrosis in LV tissue (26.8 ± 4.9% in WT vs. 36.4 ± 4.5% in cardiac DDAH1$^{-/-}$ mice, $p < 0.01$) (Fig. 2a, h).

In addition, echocardiography showed worse cardiac dysfunction in cardiac DDAH1$^{-/-}$ mice than in WT mice, with a significant decrease in EF (0.39 ± 0.05 in WT vs. 0.28 ± 0.06 in cardiac DDAH1$^{-/-}$ mice, $p < 0.01$) (Fig. 2c) and FS(19.5 ± 3.5% in WT vs. 15 ± 1.8% in cardiac DDAH1$^{-/-}$ mice, $p < 0.01$) (Fig. 2d) and an increase in the LVIDS (4.18 ± 0.25 mm in WT vs. 4.70 ± 0.20 mm in cardiac DDAH1$^{-/-}$ mice, $p < 0.01$) and LVIDD (5.18 ± 0.23 mm in WT vs. 5.50 ± 0.31 mm in cardiac DDAH1$^{-/-}$ mice, $p < 0.05$) (Fig. 2f, g).

DDAH1 deficiency promotes cardiomyocyte apoptosis and oxidative stress in LV tissue after AMI

Apoptosis was significantly enhanced in the LV tissue of cardiac DDAH1$^{-/-}$ mice (2.70 ± 0.80% in WT vs. 5.34 ± 1.29% in cardiac DDAH1$^{-/-}$ mice, $p < 0.01$) (Fig. 3a, b). Concurrently, the DHE fluorescence intensity was significantly higher in cardiac DDAH1$^{-/-}$ mice than in WT mice (1.08 ± 0.17 in WT vs. 1.84 ± 0.26 in cardiac DDAH1$^{-/-}$ mice, $p < 0.01$) (Fig. 3c, d). Western blotting

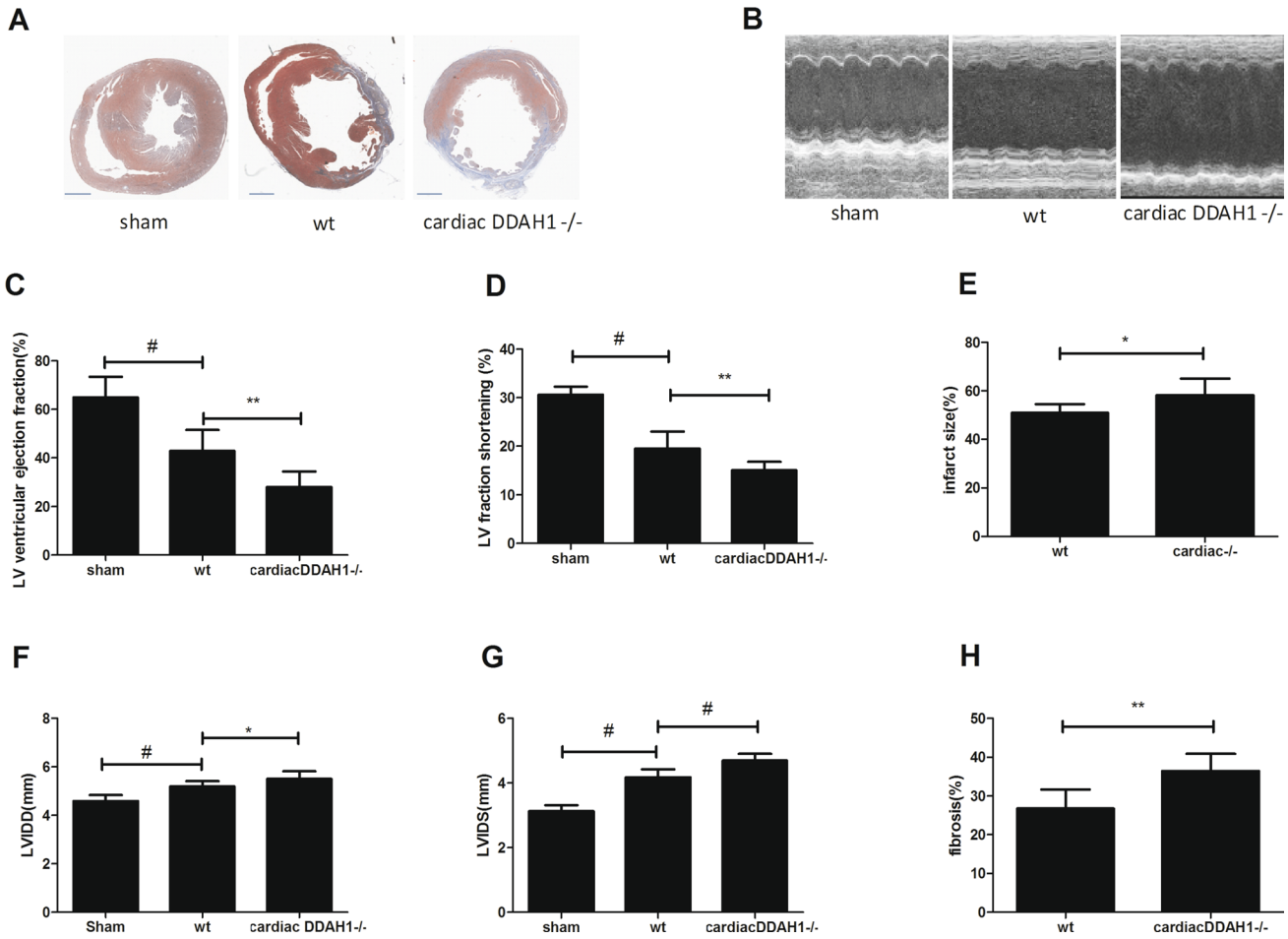

Fig. 2 DDAH1 deficiency aggravated cardiac remodeling and dysfunction after AMI. **a** Transverse sections of the mid-myocardium from WT and cardiac DDAH1$^{-/-}$ hearts post-AMI. **b** M-mode ultrasound imaging of left-ventricular structure and function. The echocardiogram shows changes in the LV ejection fraction (**c**), fractional shortening (**d**), LVIDD (**f**), and LVIDS (**g**) of WT and cardiac DDAH1$^{-/-}$ mice post-AMI. Quantitative analysis of infarct size (**e**) and fibrosis (**h**) in WT and cardiac DDAH1$^{-/-}$ hearts post-AMI. $^{*}p<0.05$, $^{**}p<0.01$, and $^{\#}p<0.001$, $n=10$–12. Scale bar = 1 mm

showed that 3-nitrotyrosine expression in LV tissue was significantly increased in cardiac DDAH1$^{-/-}$ mice compared to WT mice after AMI (1.00 ± 0.08 in WT vs. 1.90 ± 0.08 in cardiac DDAH1$^{-/-}$ mice, $p<0.01$) (Fig. 3e, f).

Cardiac DDAH1$^{-/-}$ mice had similar plasma ADMA concentrations as WT mice, and exogenous ADMA had no significant effects on cardiomyocyte apoptosis and oxidative stress

Plasma ADMA concentrations were unaffected by cardiac-specific DDAH1 deletion (0.63 ± 0.13 μmol/L in WT vs. 0.67 ± 0.06 μmol/L in cardiac DDAH1$^{-/-}$ mice) at baseline and at 7, 14, and 28 days after AMI (0.72 ± 0.11, 0.71 ± 0.08, and 0.68 ± 0.06 μmol/L in WT vs. 0.74 ± 0.13, 0.73 ± 0.09, and 0.70 ± 0.07 μmol/L in cardiac DDAH1$^{-/-}$ mice) (Fig. 4a).

We further treated WT cardiomyocytes with ADMA to study the effects of increased ADMA levels on oxidative stress and apoptosis sensitivity in cardiomyocytes. Surprisingly, the addition of exogenous ADMA (100 μM) to WT cardiomyocytes for 24 or 48 h did not exert an effect on cardiomyocyte apoptosis(2.17 ± 0.11, 2.06 ± 0.22, and 2.1 ± 0.13% for 0, 24, and 48 h, respectively) (Fig. 4b, c) and oxidative stress (1.03 ± 0.09, 1.13 ± 0.11, and 1.13 ± 0.18 for 0, 24, and 48 h, respectively) (Fig. 4d, e).

DDAH1 deficiency impaired SOD2 expression in LV tissue before and after AMI

To identify proteins related to DDAH1 deficiency-induced oxidative stress, we performed proteome analysis and found that there were 166 dysregulated proteins in the LV tissue of cardiac DDAH1$^{-/-}$ mice compared with WT mice (Fig. 5a). Among them, the expression level of the anti-oxidative

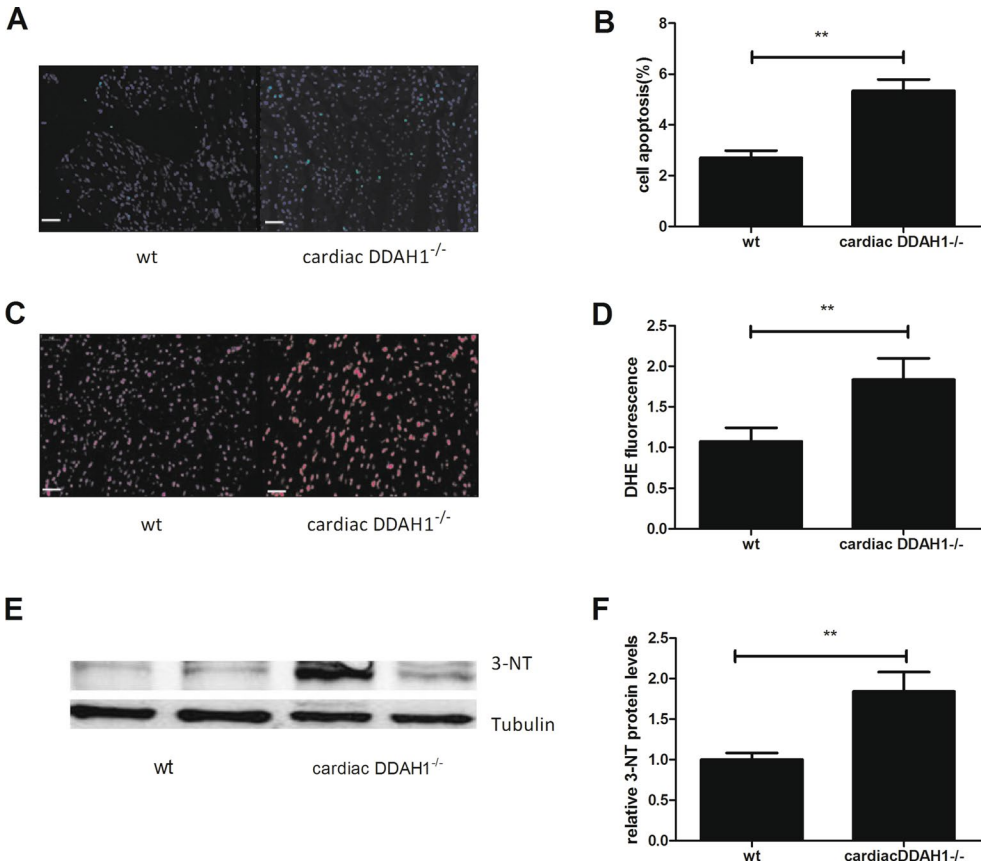

Fig. 3 DDAH1 deficiency promotes cardiomyocyte apoptosis and oxidative stress after AMI. **a** TUNEL-stained images from the border regions of WT and cardiac DDAH1$^{-/-}$ hearts post-AMI. **b** Quantitative analysis of cardiomyocyte apoptosis in the border region of WT and cardiac DDAH1$^{-/-}$ hearts post-AMI. **c** Images of DHE staining in the border regions of WT and cardiac DDAH1$^{-/-}$ hearts post-AMI. **d** Quantitative analysis of DHE fluorescence intensity in the border region of WT and cardiac DDAH1$^{-/-}$ hearts post-AMI. **e**, **f** Western blot analysis of 3-NT expression in the LV tissue of cardiac DDAH1$^{-/-}$mice compared with that of WT mice $^{*}p<0.05$, $^{**}p<0.01$, and $^{\#}p<0.001$, $n=6$. Scale bar = 50 μm

stress-related protein SOD2 was significantly reduced in the LV tissue of cardiac DDAH1$^{-/-}$ mice compared with that of WT mice after AMI (Fig. 5b, c).

Western blotting further confirmed that SOD2 expression in LV tissue was significantly reduced in cardiac DDAH1$^{-/-}$ mice compared to WT mice under baseline conditions (Fig. 6a, b, $p<0.05$). Although the SOD2 expression level was moderately increased in the LV tissue of cardiac DDAH1$^{-/-}$ mice at 4 weeks after AMI compared to baseline, it was significantly reduced in the LV tissue of cardiac DDAH1$^{-/-}$ mice compared to that of WT mice (Fig. 6a, c, $p<0.05$).

DDAH1 deficiency increased oxidative stress and promoted cardiomyocyte apoptosis under hypoxic conditions, and tempol treatment attenuated these effects

Primary cardiomyocytes from DDAH1$^{-/-}$ mice exhibited increased oxidative stress as shown by increased DHE fluorescence intensity under hypoxic conditions (Fig. 7a, b, $p<0.01$), which was restored by tempol (10 μm) treatment (Fig. 7a, b, $p<0.05$).Western blotting showed that 3-nitrotyrosine expression in cardiomyocytes from DDAH1$^{-/-}$ mice was significantly increased compared to WT mice, which was reduced by tempol treatment (Fig. 7c, d, $p<0.01$).

Under hypoxic conditions, primary cardiomyocytes from DDAH1$^{-/-}$ mice also showed a higher rate of apoptosis, as assessed by TUNEL staining, compared to cardiomyocytes from WT mice (Fig. 7e, f, $p<0.01$); however, tempol (10 μm) treatment ameliorated this change in cardiomyocyte apoptosis (Fig. 7e, f, $p<0.05$).

Treatment of cardiac DDAH1$^{-/-}$ mice with tempol attenuated oxidative stress and apoptosis in LV tissue after AMI

DHE staining was significantly reduced after tempol (1.5 mmol/kg/day) treatment in cardiac DDAH1$^{-/-}$ mice compared to PBS-treated mice after AMI (Fig. 8a, b, $p<0.01$). Western blotting showed that 3-nitrotyrosine expression in LV tissue was significantly reduced after tempol (1.5 mmol/kg/day) treatment in cardiac DDAH1$^{-/-}$ mice compared to PBS-treated mice after AMI (Fig. 8c, d, $p<0.01$).

Importantly, tempol treatment significantly decreased apoptosis in the LV tissue of cardiac DDAH1$^{-/-}$mice after AMI (Fig. 8e, f, $p<0.01$).

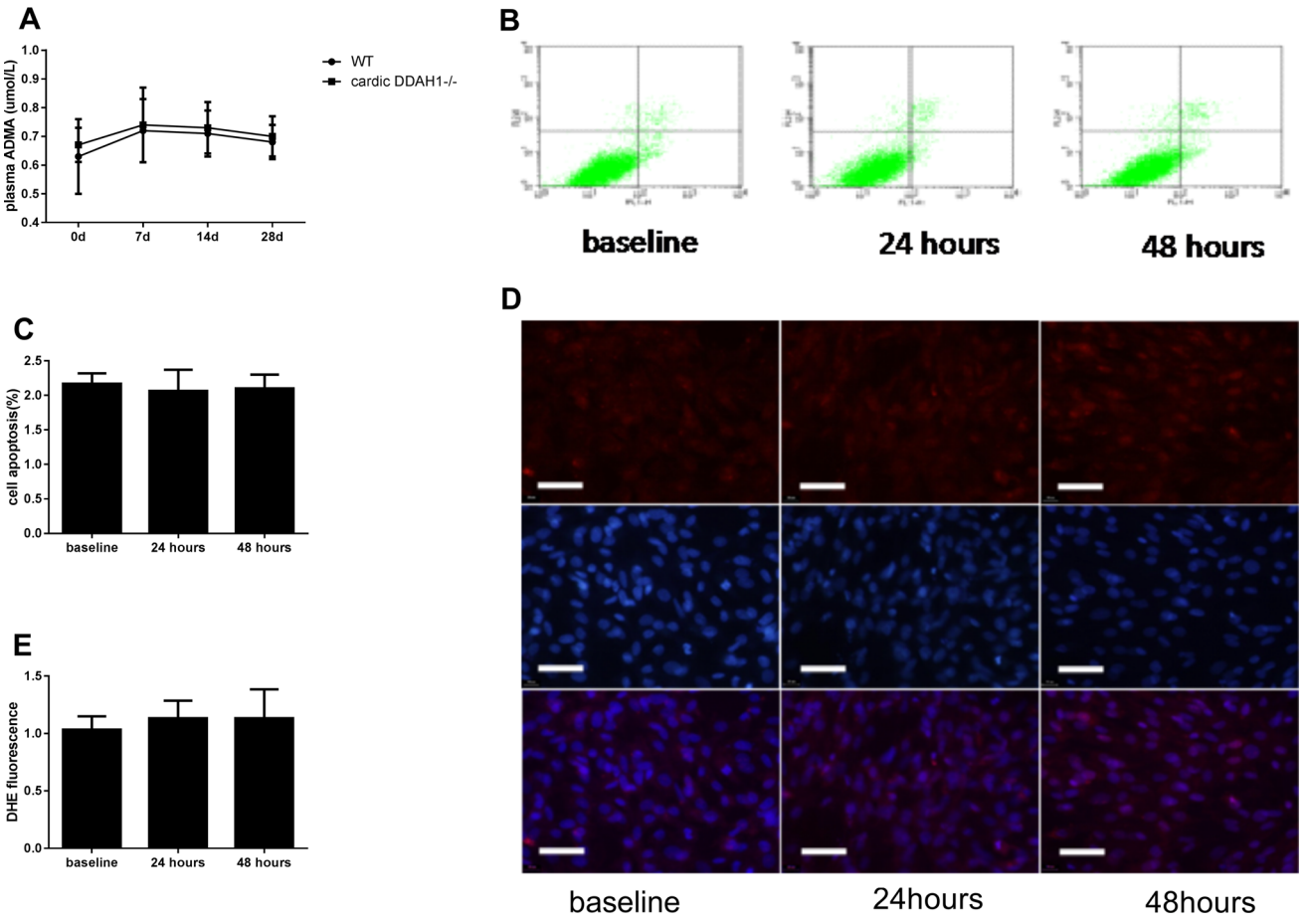

Fig. 4 Effects of DDAH1 deficiency on plasma ADMA levels and exogenous ADMA on cardiomyocyte apoptosis or oxidative stress. **a** Plasma ADMA level in WT mice and cardiac DDAH1$^{-/-}$ mice before and after AMI; $n=10$. **b**, **c** Flow cytometry analysis of the effect of exogenous ADMA on cardiomyocyte apoptosis. **d** Quantitative analysis of DHE fluorescence intensity in ADMA-treated cardiomyocytes. **e** Image of DHE-stained cardiomyocytes treated with ADMA. Scale bar = 50 μm

Treatment of cardiac DDAH1$^{-/-}$ mice with tempol effectively rescued LV remodeling after AMI

Compared to PBS, tempol (1.5 mmol/kg/day) treatment significantly rescued the LV EF (0.28 ± 0.07 vs. 0.34 ± 0.04, $p < 0.05$) (Fig. 9a) and FS (15.8 ± 2.3 vs. $17.4 \pm 2.0\%$, $p < 0.01$) (Fig. 9b) in cardiac DDAH1$^{-/-}$ mice at 4 weeks after AMI; however, no significant effect on WT mice was observed (Fig. 9a, b). Both the LVIDD (5.48 ± 0.19 vs. 5.28 ± 0.28 mm, $p < 0.05$) (Fig. 9c) and LVIDS (4.70 ± 0.20 vs. 4.36 ± 0.22 mm, $p < 0.01$) (Fig. 9d) were reduced in cardiac DDAH1$^{-/-}$ mice. Infarct size (60.05 ± 5.69 vs. $54.59 \pm 7.04\%$, $p = 0.11$) (Fig. 9e) and LV fibrosis (36.38 ± 4.50 vs. $32.50 \pm 3.16\%$, $p = 0.07$) (Fig. 9f) were reduced with tempol treatment in cardiac DDAH1$^{-/-}$ mice, although the differences were not statistically significant.

Discussion

The major finding of the present study is that cardiac-specific deletion of DDAH1 exacerbates the LV remodeling and dysfunction induced by AMI through increasing oxidative stress and cardiomyocyte apoptosis. The mechanism underlying this process is partly due to miR-21-induced decreases in the SOD2 expression level rather than local ADMA accumulation.

DDAH1 is a critical enzyme for ADMA degradation and is expressed in several tissues and cell types, including hepatocytes, renal tubular cells, neurocytes, and adipocytes [11, 13, 14, 17, 25, 26]. The previous studies have confirmed that global deletion of DDAH1 leads to significantly elevated plasma ADMA levels [5, 11] and that increased plasma ADMA is an independent risk factor for cardiovascular diseases [2]. Recently, Chen and

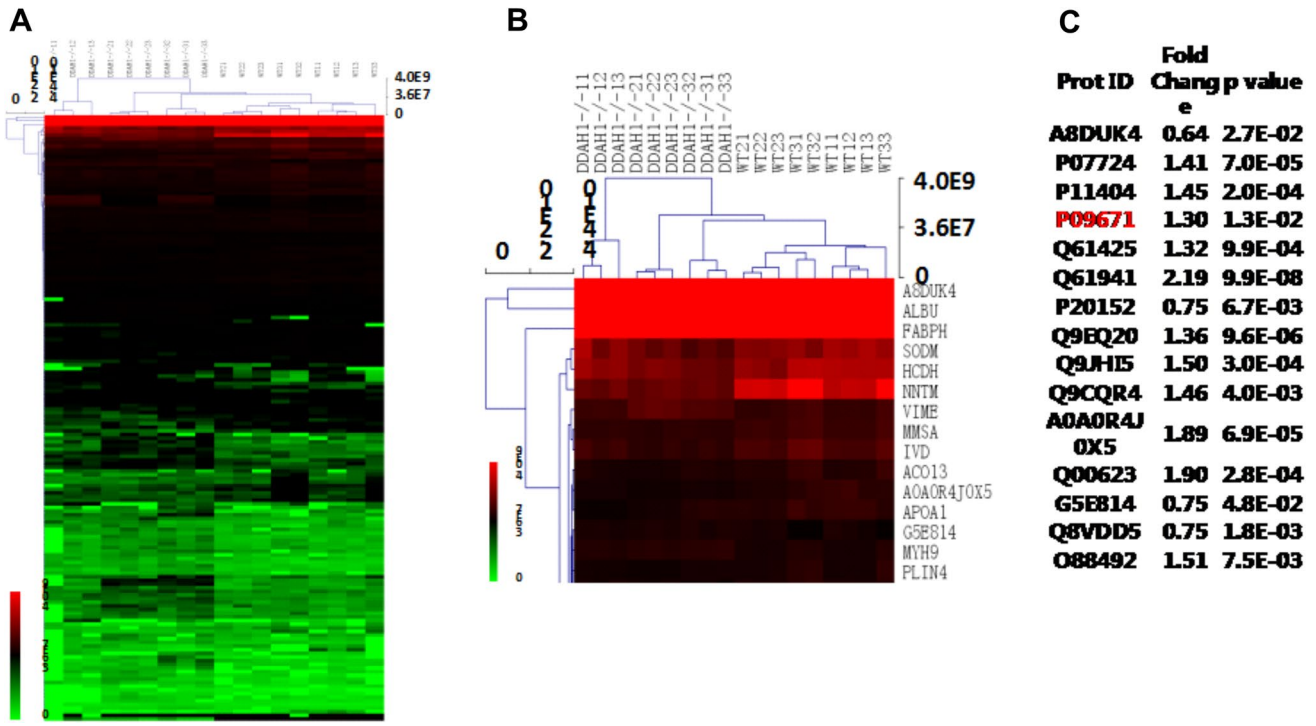

Fig. 5 Proteome analysis of LV tissue of cardiac DDAH1$^{-/-}$ mice and WT mice. **a** Hierarchical clustering analysis of 166 dysregulated proteins in the LV tissue of cardiac DDAH1$^{-/-}$ mice compared with that of WT mice. **b** and **c** Hierarchical clustering analysis of the top 15 proteins in the LV tissue of cardiac DDAH1$^{-/-}$ mice compared with that of WT mice; $n=3$

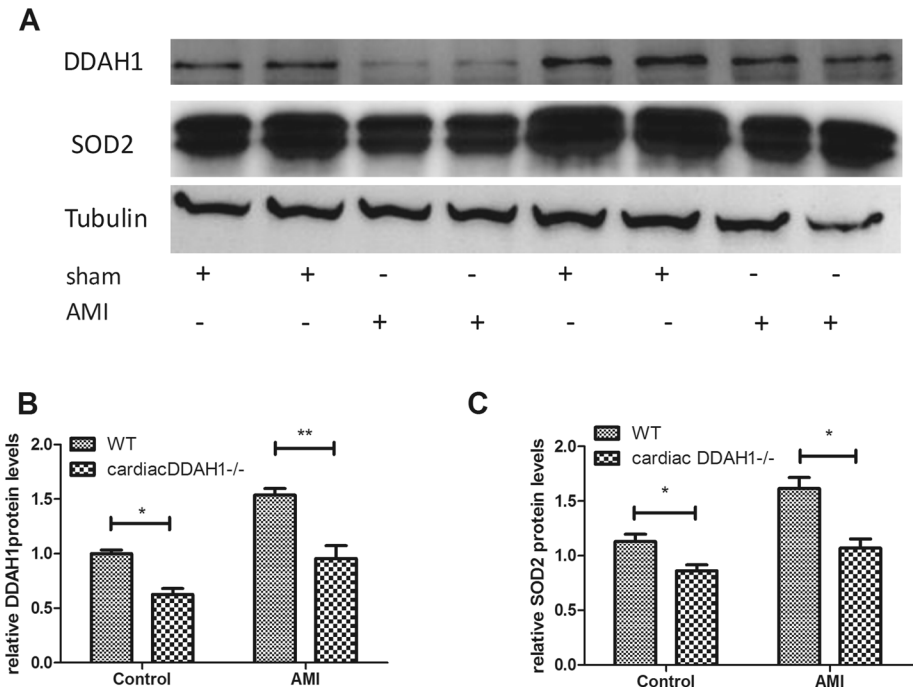

Fig. 6 DDAH1 deficiency reduces SOD2 expression in LV tissues. **a** Western blot analysis confirmed changes in DDAH1 and SOD2 expression in the LV tissue of WT and cardiac DDAH1$^{-/-}$ mice before and after AMI. **b** Quantitative analysis of DDAH1 expression in the LV tissue of WT and cardiac DDAH1$^{-/-}$ mice before and after AMI. **c** Quantitative analysis of SOD2 expression in the LV tissue of WT and cardiac DDAH1$^{-/-}$ mice before and after AMI. $^{*}p<0.05$, $^{**}p<0.01$, and $^{\#}p<0.001$; $n=6$

his colleagues found that cardiomyocyte DDAH1 activity was dispensable for cardiac function under basal conditions but played an important role in attenuating cardiac hypertrophy and ventricular remodeling under stress conditions. However, the exact mechanism underlying the protective role of DDAH1 in cardiomyocytes was unclear. The authors speculated that oxidative stress might be the chief culprit, as evidenced by dramatically increased

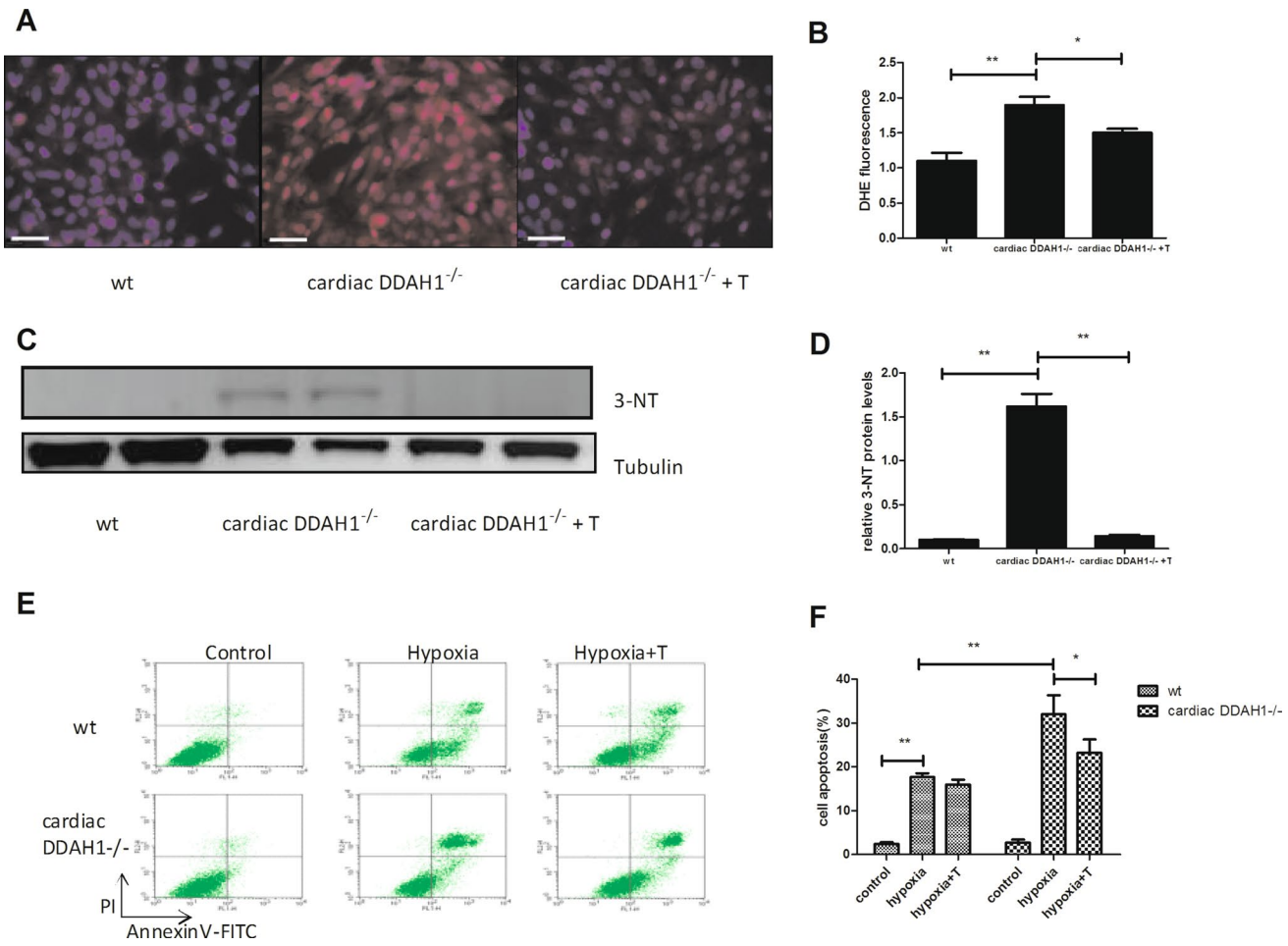

Fig. 7 Tempol treatment attenuated cardiomyocytes oxidative stress and apoptosis increased by DDAH1 deficiency under hypoxic conditions. **a** Images of DHE-stained cardiomyocytes from WT and DDAH1$^{-/-}$ mice cultured under hypoxic conditions. **b** Quantitative analysis of DHE fluorescence intensity in cardiomyocytes from WT and DDAH1$^{-/-}$ mice cultured under hypoxic conditions. **c**, **d** Western blot analysis of 3-NT expression in cardiomyocytes from WT and DDAH1$^{-/-}$ mice cultured under hypoxic conditions. **e** and **f** Flow cytometry analysis of apoptosis in cardiomyocytes from WT and DDAH1$^{-/-}$ mice cultured under hypoxic conditions. $^{*}p<0.05$, $^{**}p<0.01$, and $^{\#}p<0.001$. Scale bar = 50 μm

expression levels of 3-nitrotyrosine in the LV tissue of cardiac DDAH1$^{-/-}$ mice compared with that of WT mice in the context of transverse aortic constriction (TAC) [28].

Oxidative stress plays a major role in the initiation and progression of the cardiac structural and functional abnormalities observed in heart failure [15, 24]. Abundant evidence has confirmed the presence of oxidative stress-mediated cardiomyocyte apoptosis in several heart models [8, 16]. The previous studies have showed that stimulating glucose oxidation or altering fatty acid oxidation rates can improve heart remodeling and cardiac function in human heart failure [9]. Paroxetine treatment following MI decreased LV remodeling and susceptibility to arrhythmias, while reducing ROS formation [15]. Restoration of oxidative stress homeostasis is believed to be a promising therapeutic strategy to treat heart remodeling and failure after AMI.

The present study found that the cardiomyocyte-specific deletion of DDAH1 did not affect plasma ADMA levels after AMI, suggesting that cardiomyocytes are not the major sources of systemic ADMA and that cardiomyocyte DDAH1 exerts systemic ADMA-independent protective effects on LV remodeling and dysfunction after AMI. As a previous study showed, the tissue ADMA level in cardiac DDAH1$^{-/-}$ mice was moderately increased compared to that in WT mice under stress conditions [28]. Moreover, we studied the effect of ADMA on the cultured cardiomyocytes and found that exogenous ADMA did not exert a significant effect on oxidative stress or apoptosis in cardiomyocytes. The above results suggest that cardiomyocyte-specific deletion of DDAH1 can aggravate LV remodeling after AMI independent of the exogenous ADMA level.

MnSOD (SOD2) is an essential antioxidant protein located in the mitochondrial matrix. One important role of

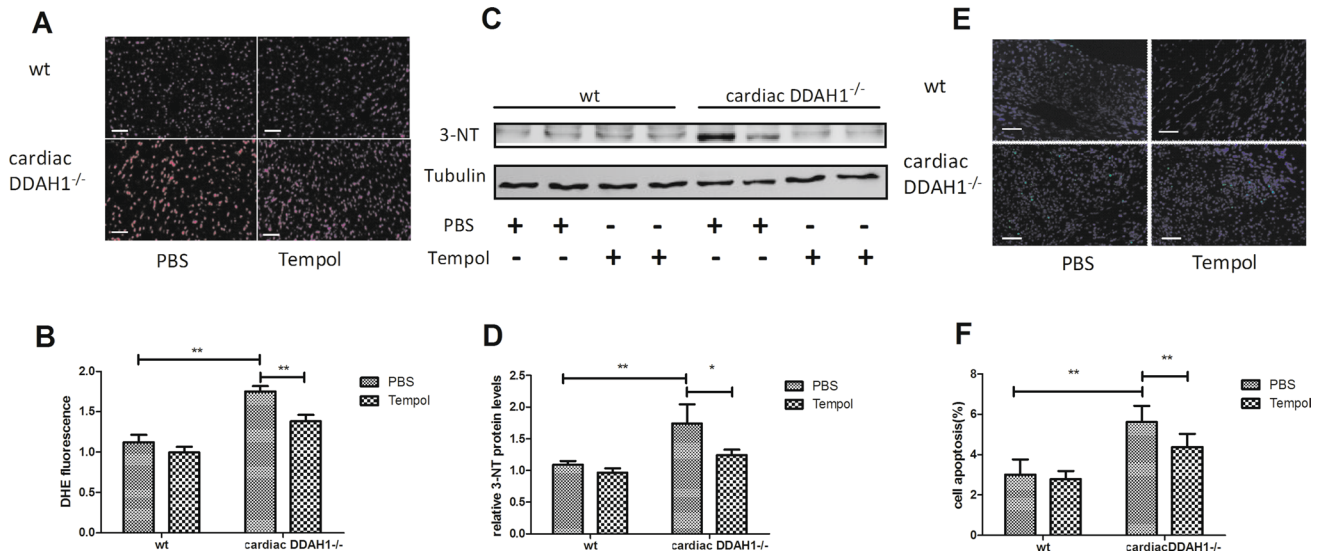

Fig. 8 Tempol treatment attenuated oxidative stress and apoptosis in the LV tissue of cardiac DDAH1$^{-/-}$ mice after AMI. **a** Images of DHE-stained WT and cardiac DDAH1$^{-/-}$ heart tissue post-AMI and after tempol treatment. **b** Quantitative analysis of DHE fluorescence intensity in WT and cardiac DDAH1$^{-/-}$ heart tissues post-AMI and after tempol treatment. **c**, **d** Western blot analysis of 3-NT expression in WT and cardiac DDAH1$^{-/-}$ hearts post-AMI and after tempol treatment. **e** Images of TUNEL-stained WT and cardiac DDAH1$^{-/-}$ hearts post-AMI and after tempol treatment. **f** Quantitative analysis of cardiomyocyte apoptosis in WT and cardiac DDAH1$^{-/-}$ hearts post-AMI and after tempol treatment. *$p<0.05$ and **$p<0.01$; $n=6$. Scale bar = 50 µm

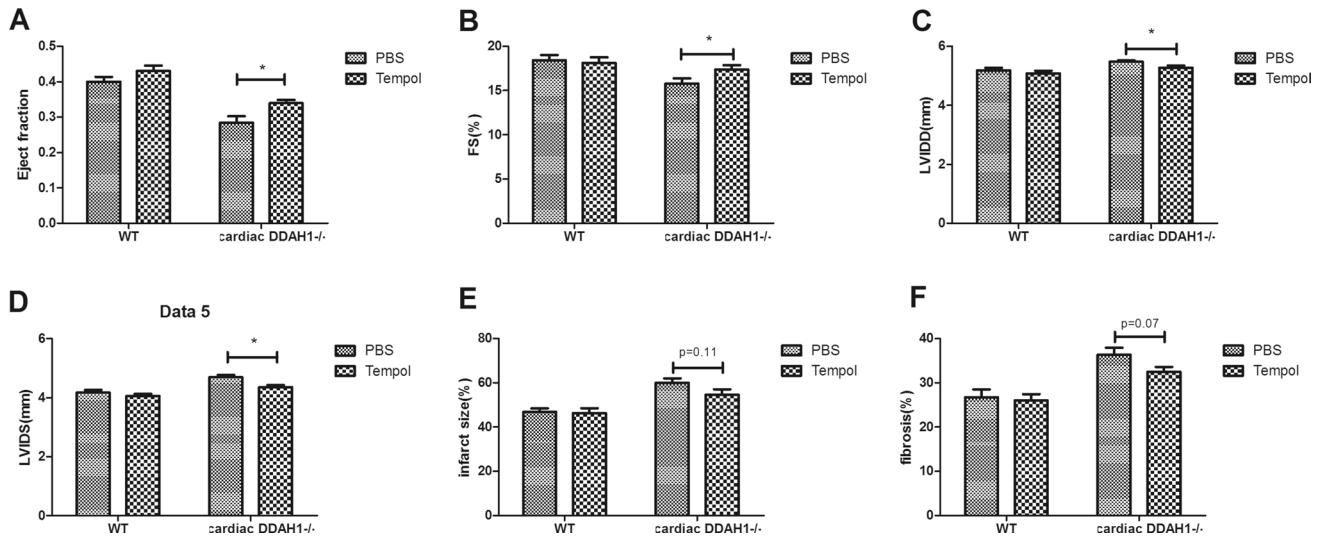

Fig. 9 Tempol treatment alleviated LV remodeling in cardiac DDAH1$^{-/-}$ mice after AMI echocardiogram shows the rescue effects of tempol on the LV ejection fraction (**a**), fractional shortening (**b**), LVIDD (**c**), and LVIDS (**d**) of WT and cardiac DDAH1$^{-/-}$ mouse hearts post-AMI. Quantitative analysis of infarct size (**e**) and fibrosis (**f**) in WT and cardiac DDAH1$^{-/-}$ post-AMI hearts after tempol treatment. *$p<0.05$ and **$p<0.01$; $n=10$–12

SOD2 is to catalyze the dismutation of superoxide anions to hydrogen peroxide [10, 18]. The previous studies have shown a significant oxidative damage to mitochondria in SOD2$^{-/+}$ mice compared to WT mice [21]. In contrast, SOD2 overexpression in mice may protect against oxidative stress, apoptosis, and fibrosis [20]. In this study, we found that SOD2 expression was significantly reduced in the LV tissue of cardiac DDAH1$^{-/-}$ mice compared to that of WT mice under baseline conditions, which indicated that DDAH1 in cardiomyocytes might regulate the expression of SOD2 in cardiomyocytes. Furthermore, we found that, while the level of SOD2 increased dramatically in WT mice after AMI, the level of SOD2 was rather low in the LV tissue of cardiac DDAH1$^{-/-}$ mice compared to that of

WT mice. Recent study showed that DDAH1 deficiency impaired the expression of SOD2 in mouse embryonic fibroblasts [29], and our study confirmed, for the first time, the effect of DDAH1 deficiency on SOD2 expression in cardiomyocytes. These findings combined with those of previous studies showed that increased SOD2 expression after AMI might represent a homeostatic response aimed at reducing the intensity of ischemic injury. These findings were also comparable to the results of studies by Wang and others who showed that SOD2 was involved in oxidative stress homeostasis regulation during the early reperfusion after AMI [27].

However, DDAH1 deficiency impaired the homeostatic response, increased oxidative stress-related apoptosis, and led to aggravated LV remodeling in cardiac DDAH1$^{-/-}$ mice.

Further in vitro experiments showed that DDAH1 deficiency promoted oxidative stress and apoptosis in cardiomyocytes under hypoxic conditions, and that these effects could be attenuated by tempol, a superoxide dismutase mimetic, thereby supporting the correlation between DDAH1 deficiency-induced SOD2 downregulation and cardiomyocyte oxidative stress and apoptosis. These findings indicated that SOD2 may play a crucial role in the cardiac-specific DDAH1 deficiency-induced LV remodeling and dysfunction after AMI.

To confirm the above findings, we performed rescue experiments and found that treatment of cardiac DDAH1$^{-/-}$ mice with tempol significantly attenuated oxidative stress and apoptosis in cardiomyocytes and rescued LV function, as demonstrated by the increased EF and FS. However, treatment of WT mice with tempol failed to mitigate the LV remodeling caused by AMI. This finding is reasonable, as the SOD2 level in WT AMI mice increased sufficiently to maintain oxidative/anti-oxidative stress homeostasis after AMI, whereas cardiac DDAH1$^{-/-}$ mice lost the ability to reestablish balance and needed the exogenous SOD mimic tempol to restore the homeostatic response. Tempol is an SOD mimic widely used in the previous studies, as it promotes $O2^-$ metabolism at rates that are similar to SOD. Although tempol also promotes the metabolism of other ROS and reactive nitrogen species, which may contribute to the rescue effects of tempol, proteome analysis in our study did not reveal significant changes in any redox-active enzyme other than SOD2, suggesting that cardiac DDAH1 deficiency causes oxidative stress injury. Furthermore, any other potential effect from tempol would be consistent among groups, and we did not observe a significant beneficial effect from tempol treatment on WT mice after AMI. Therefore, it is possible that tempol exerted a rescue effect in our study because of its SOD mimic characteristic.

Although tempol significantly improved the EF and FS of cardiac DDAH1$^{-/-}$ AMI mice, the rescue effects were not as distinct as expected. This is reasonable, as DDAH1 deficiency can not only reduce SOD2 expression levels but also increase local ADMA levels, as we mentioned above. Moreover, chronic ADMA accumulation can impair endothelial cell function and reduce angiogenesis in an SOD2-independent manner, which can aggravate LV remodeling after AMI and cannot be rescued by SOD mimic treatment.

Conclusions

Cardiomyocyte DDAH1 attenuates LV remodeling after AMI by reducing the ROS level and apoptosis sensitivity in cardiomyocytes, at least partly, by regulating SOD2 expression.

Acknowledgements We thank Prof. Professor Yinjie Chen from the University of Minnesota for kindly offering DDAH1$^{-/-}$ mice and valued advice for this study.

Funding This study was supported by research Grants 81770254, 81600308 from National Natural Science Foundation of China.

Compliance with ethical standards

Conflict of interest All authors declare that they have no competing interests.

References

1. Anderssohn M, Schwedhelm E, Luneburg N, Vasan RS, Boger RH (2010) Asymmetric dimethylarginine as a mediator of vascular dysfunction and a marker of cardiovascular disease and mortality: an intriguing interaction with diabetes mellitus. Diab Vasc Dis Res 7:105–118. https://doi.org/10.1177/1479164110366053
2. Boger RH (2006) Asymmetric dimethylarginine (ADMA): a novel risk marker in cardiovascular medicine and beyond. Ann Med 38:126–136. https://doi.org/10.1080/07853890500472151
3. Boger RH, Sullivan LM, Schwedhelm E, Wang TJ, Maas R, Benjamin EJ, Schulze F, Xanthakis V, Benndorf RA, Vasan RS (2009) Plasma asymmetric dimethylarginine and incidence of cardiovascular disease and death in the community. Circulation 119:1592–1600. https://doi.org/10.1161/CIRCULATIONAHA.108.838268
4. Chirinos JA, Akers SR, Trieu L, Ischiropoulos H, Doulias PT, Tariq A, Vassim I, Koppula MR, Syed AA, Soto-Calderon H, Townsend RR, Cappola TP, Margulies KB, Zamani P (2016) Heart failure, left ventricular remodeling, and circulating nitric oxide metabolites. J Am Heart Assoc. https://doi.org/10.1161/JAHA.116.004133
5. Dowsett L, Piper S, Slaviero A, Dufton N, Wang Z, Boruc O, Delahaye M, Colman L, Kalk E, Tomlinson J, Birdsey G, Randi AM, Leiper J (2015) Endothelial dimethylarginine dimethylaminohydrolase 1 is an important regulator of angiogenesis but does not regulate vascular reactivity or hemodynamic homeostasis. Circulation 131:2217–2225. https://doi.org/10.1161/CIRCULATIONAHA.114.015064
6. Guellich A, Damy T, Conti M, Claes V, Samuel JL, Pineau T, Lecarpentier Y, Coirault C (2013) Tempol prevents cardiac oxidative damage and left ventricular dysfunction in the PPAR-alpha KO mouse. Am J Physiol Heart Circ Physiol 304:H1505–H1512. https://doi.org/10.1152/ajpheart.00669.2012

7. Guo JJ, Ma LL, Shi HT, Zhu JB, Wu J, Ding ZW, An Y, Zou YZ, Ge JB (2016) Alginate oligosaccharide prevents acute doxorubicin cardiotoxicity by suppressing oxidative stress and endoplasmic reticulum-mediated apoptosis. Mar Drugs. https://doi.org/10.3390/md14120231
8. Hashem SI, Perry CN, Bauer M, Han S, Clegg SD, Ouyang K, Deacon DC, Spinharney M, Panopoulos AD, Izpisua Belmonte JC, Frazer KA, Chen J, Gong Q, Zhou Z, Chi NC, Adler ED (2015) Brief report: oxidative stress mediates cardiomyocyte apoptosis in a human model of danon disease and heart failure. Stem Cells 33:2343–2350. https://doi.org/10.1002/stem.2015
9. Heusch G, Libby P, Gersh B, Yellon D, Bohm M, Lopaschuk G, Opie L (2014) Cardiovascular remodelling in coronary artery disease and heart failure. Lancet 383:1933–1943. https://doi.org/10.1016/S0140-6736(14)60107-0
10. Holley AK, Dhar SK, Xu Y, St Clair DK (2012) Manganese superoxide dismutase: beyond life and death. Amino Acids 42:139–158. https://doi.org/10.1007/s00726-010-0600-9
11. Hu X, Xu X, Zhu G, Atzler D, Kimoto M, Chen J, Schwedhelm E, Luneburg N, Boger RH, Zhang P, Chen Y (2009) Vascular endothelial-specific dimethylarginine dimethylaminohydrolase-1-deficient mice reveal that vascular endothelium plays an important role in removing asymmetric dimethylarginine. Circulation 120:2222–2229. https://doi.org/10.1161/CIRCULATIONAHA.108.819912
12. Hu X, Atzler D, Xu X, Zhang P, Guo H, Lu Z, Fassett J, Schwedhelm E, Boger RH, Bache RJ, Chen Y (2011) Dimethylarginine dimethylaminohydrolase-1 is the critical enzyme for degrading the cardiovascular risk factor asymmetrical dimethylarginine. Arterioscler Thromb Vasc Biol 31:1540–1546. https://doi.org/10.1161/ATVBAHA.110.222638
13. Iannone L, Zhao L, Dubois O, Duluc L, Rhodes CJ, Wharton J, Wilkins MR, Leiper J, Wojciak-Stothard B (2014) miR-21/DDAH1 pathway regulates pulmonary vascular responses to hypoxia. Biochem J 462:103–112. https://doi.org/10.1042/BJ20140486
14. Kim HY, Kim JH, Kim HS (2013) Effect of CCL5 on dimethylarginine dimethylaminohydrolase-1 production in vascular smooth muscle cells from spontaneously hypertensive rats. Cytokine 64:227–233. https://doi.org/10.1016/j.cyto.2013.06.316
15. Lassen TR, Nielsen JM, Johnsen J, Ringgaard S, Botker HE, Kristiansen SB (2017) Effect of paroxetine on left ventricular remodeling in an in vivo rat model of myocardial infarction. Basic Res Cardiol 112:26. https://doi.org/10.1007/s00395-017-0614-5
16. Munzel T, Camici GG, Maack C, Bonetti NR, Fuster V, Kovacic JC (2017) Impact of oxidative stress on the heart and vasculature: part 2 of a 3-part series. J Am Coll Cardiol 70:212–229. https://doi.org/10.1016/j.jacc.2017.05.035
17. Onozato ML, Tojo A, Leiper J, Fujita T, Palm F, Wilcox CS (2008) Expression of NG, NG-dimethylarginine dimethylaminohydrolase and protein arginine N-methyltransferase isoforms in diabetic rat kidney: effects of angiotensin II receptor blockers. Diabetes 57:172–180. https://doi.org/10.2337/db06-1772
18. Raha S, McEachern GE, Myint AT, Robinson BH (2000) Superoxides from mitochondrial complex III: the role of manganese superoxide dismutase. Free Radic Biol Med 29:170–180
19. Roger VL, Go AS, Lloyd-Jones DM, Benjamin EJ, Berry JD, Borden WB, Bravata DM, Dai S, Ford ES, Fox CS, Fullerton HJ, Gillespie C, Hailpern SM, Heit JA, Howard VJ, Kissela BM, Kittner SJ, Lackland DT, Lichtman JH, Lisabeth LD, Makuc DM, Marcus GM, Marelli A, Matchar DB, Moy CS, Mozaffarian D, Mussolino ME, Nichol G, Paynter NP, Soliman EZ, Sorlie PD, Sotoodehnia N, Turan TN, Virani SS, Wong ND, Woo D, Turner MB (2012) Executive summary: heart disease and stroke statistics—2012 update: a report from the American Heart Association. Circulation 125:188–197. https://doi.org/10.1161/CIR.0b013e3182456d46
20. Silva JP, Shabalina IG, Dufour E, Petrovic N, Backlund EC, Hultenby K, Wibom R, Nedergaard J, Cannon B, Larsson NG (2005) SOD2 overexpression: enhanced mitochondrial tolerance but absence of effect on UCP activity. EMBO J 24:4061–4070. https://doi.org/10.1038/sj.emboj.7600866
21. Strassburger M, Bloch W, Sulyok S, Schuller J, Keist AF, Schmidt A, Wenk J, Peters T, Wlaschek M, Lenart J, Krieg T, Hafner M, Kumin A, Werner S, Muller W, Scharffetter-Kochanek K (2005) Heterozygous deficiency of manganese superoxide dismutase results in severe lipid peroxidation and spontaneous apoptosis in murine myocardium in vivo. Free Radic Biol Med 38:1458–1470. https://doi.org/10.1016/j.freeradbiomed.2005.02.009
22. Sun X, Zhang H, Luo L, Zhong K, Ma Y, Fan L, Fu D, Wan L (2016) Comparative proteomic profiling identifies potential prognostic factors for human clear cell renal cell carcinoma. Oncol Rep 36:3131–3138. https://doi.org/10.3892/or.2016.5159
23. Toischer K, Zhu W, Hunlich M, Mohamed BA, Khadjeh S, Reuter SP, Schafer K, Ramanujam D, Engelhardt S, Field LJ, Hasenfuss G (2017) Cardiomyocyte proliferation prevents failure in pressure overload but not volume overload. J Clin Invest 127:4285–4296. https://doi.org/10.1172/JCI81870
24. Tomczyk M, Kraszewska I, Szade K, Bukowska-Strakova K, Meloni M, Jozkowicz A, Dulak J, Jazwa A (2017) Splenic Ly6C(hi) monocytes contribute to adverse late post-ischemic left ventricular remodeling in heme oxygenase-1 deficient mice. Basic Res Cardiol 112:39. https://doi.org/10.1007/s00395-017-0629-y
25. Tran CT, Fox MF, Vallance P, Leiper JM (2000) Chromosomal localization, gene structure, and expression pattern of DDAH1: comparison with DDAH2 and implications for evolutionary origins. Genomics 68:101–105. https://doi.org/10.1006/geno.2000.6262
26. Wang S, Hu CP, Yuan Q, Zhang WF, Zhou Z, Nie SD, Jiang JL, Li YJ (2012) Dimethylarginine dimethylaminohydrolase 1 regulates nerve growth factor-promoted differentiation of PC12 cells in a nitric oxide-dependent but asymmetric dimethylargenine-independent manner. J Neurosci Res 90:1209–1217. https://doi.org/10.1002/jnr.23009
27. Wang XX, Wang XL, Tong MM, Gan L, Chen H, Wu SS, Chen JX, Li RL, Wu Y, Zhang HY, Zhu Y, Li YX, He JH, Wang M, Jiang W (2016) SIRT6 protects cardiomyocytes against ischemia/reperfusion injury by augmenting FoxO3alpha-dependent antioxidant defense mechanisms. Basic Res Cardiol 111:13. https://doi.org/10.1007/s00395-016-0531-z
28. Xu X, Zhang P, Kwak D, Fassett J, Yue W, Atzler D, Hu X, Liu X, Wang H, Lu Z, Guo H, Schwedhelm E, Boger RH, Chen P, Chen Y (2017) Cardiomyocyte dimethylarginine dimethylaminohydrolase-1 (DDAH1) plays an important role in attenuating ventricular hypertrophy and dysfunction. Basic Res Cardiol 112:55. https://doi.org/10.1007/s00395-017-0644-z
29. Zhao C, Li T, Han B, Yue W, Shi L, Wang H, Guo Y, Lu Z (2016) DDAH1 deficiency promotes intracellular oxidative stress and cell apoptosis via a miR-21-dependent pathway in mouse embryonic fibroblasts. Free Radic Biol Med 92:50–60. https://doi.org/10.1016/j.freeradbiomed.2016.01.015